Pharmacogn J. 2025; 17(6): 676-682
A Multifaceted Journal in the field of Natural Products and Pharmacognosy
www.phcogj.com

Original Article

Characterization of Green Synthesized Silver Nanoparticles from *Clerodendrum thomsoniae* Balf.f., and Their Antioxidant and Anti inflammatory Potential

Pallab Kar[1]*, Ayodeji O. Oriola[2]*, Adebola O. Oyedeji[1,2]

ABSTRACT

Introduction: Medicinal plant extracts and other natural products have continued to find useful applications in nanomedicines due to their interesting biological properties. *Clerodendrum thomsoniae* (CT) is a plant used in traditional medicine to treat stress- and inflammation-related diseases, including jaundice, diabetes, and cancer. **Objectives:** This study, therefore, evaluated CT extract-based silver nanoparticles (Ag NPs) for their antioxidant and anti-inflammatory potential. **Materials and Methods:** The nanoparticles were prepared using green synthesis methods. They were characterized using UV-Vis spectroscopy, scanning electron microscopy (SEM), field emission scanning electron microscopy (FESEM), energy-dispersive X-ray spectroscopy (EDX), and X-ray diffraction (XRD). Antioxidant study was based on NO, H2O2, superoxide, and hydroxyl radical scavenging spectrophotometric methods. The *in vitro* anti-inflammatory test was based on a protein (egg albumin) denaturation assay. **Results:** Results showed CT-Ag NPs ranged from spherical to cubic shapes. The UV absorption peak at 427 nm suggests CT-Ag NP formation. The presence of elemental Ag (96.04 %) by EDX analysis suggests the conversion of metallic silver into elemental silver. The crystallinity of the nanoparticles was shown on the X-ray diffractogram as a sharp peak at 38.12° [reflection index (111)] with an average particle size of 47 nm. CT-Ag NPs showed dose-dependent hydroxyl and nitric oxide radical scavenging activities with 67.63 ± 0.78 % and 58.48 ± 1.20 %, respectively, at 200 µg/mL. It showed a notable anti-inflammatory effect by inhibiting protein denaturation with an IC50 of 53.58 ± 17.78 µg/mL. **Conclusions**: It can be deduced from this study that CT-Ag NPs show promise as antioxidant and anti-inflammatory agents.
Keywords: *Clerodendrum thomsoniae;* silver nanoparticles; antioxidant; anti-inflammatory

Pallab Kar[1]*, Ayodeji O. Oriola[2]*, Adebola O. Oyedeji[1,2]

[1]*African Medicinal Flora and Fauna Research Niche, Walter Sisulu University, Nelson Mandela Drive, P/Bag X1, Mthatha 5117, SOUTH AFRICA.*

[2]*Department of Chemical and Physical Sciences, Walter Sisulu University, Nelson Mandela Drive, P/Bag X1, Mthatha 5117, SOUTH AFRICA.*

Correspondence

K. Pallab, A. O. Oriola

African Medicinal Flora and Fauna Research Niche, Walter Sisulu University, Nelson Mandela Drive, P/Bag X1, Mthatha 5117, SOUTH AFRICA.

Department of Chemical and Physical Sciences, Walter Sisulu University, Nelson Mandela Drive, P/Bag X1, Mthatha 5117, SOUTH AFRICA

E-mail: pallabkar.bio@gmail.com & aoriola@wsu.ac.za

History

- Submission Date: 17-10-2025;
- Review completed: 04-11-2025;
- Accepted Date: 19-11-2025.

DOI : 10.5530/pj.2025.17.84

Article Available online

http://www.phcogj.com/v17/i6

INTRODUCTION

Nanotechnology has become a rapidly growing field in materials science. Over the past fifty years, material scientists have been investigating the different uses of nanoparticles (NPs) and nanostructured materials in the healthcare and biomedical sectors[1]. The form, size, and distribution of the nanoparticles can all influence their novel or improved characteristics. Recent years have seen considerable advancements in the field of nanotechnology, and a number of techniques have been developed to create precisely sized and shaped nanoparticles in accordance with specific criteria[2]. Applications for nanomaterials and nanoparticles are growing daily. Nanoparticles are very different from the bulk form of the same material because of their small size, which creates new opportunities for biosensors, biomedicine, and bionanotechnology[3]. NPs can be produced by a variety of physical and chemical processes, including thermal decomposition, chemical reduction, laser ablation, ultrasonication, electrochemical-assisted synthesis, and others. However, many of these procedures are costly and involve the use of hazardous chemicals that may pose a major risk to human health and the environment. In recent years, biological techniques have been the preferred synthesis method for producing NPs because of their relative safety, cost, and environmental friendliness[4].

The most promising nanomaterials for biological applications in recent years are silver nanoparticles (AgNPs), especially as innovative antibacterial, antioxidant, anticancer, larvicidal, catalytic, and wound healing activities[5]. Secondary metabolites from medicinal plants, such as sugars, polysaccharides, alkaloids, and flavonoids, have been shown to be quite useful when synthesizing nanoparticles. The genus *Clerodendrum* has been implicated in various traditional medicine systems for the treatment of various life-threatening diseases. The medicinal plant *Clerodendrum thomsoniae* Balf.f., often known as the bleeding-heart vine or bag flower, is an ornamental vine used in Indian and Japanese traditional systems to treat a variety of severe ailments, such as cancer, typhoid, syphilis, jaundice, and hypertension[6]. It is a member of the genus Clerodendrum and the family Lamiaceae[6]. *Clerodendrum thomsoniae* is found in large numbers in America, Africa, Australia, and Asia[7]. Traditional healers in Cameroon employ *C. thomsoniae* as a folk medicine to cure obesity and diabetes. Fatty acids (linoleic acid, palmitic, and heptadecanoic acid) and phytosterols (stigmasterol and α-tocopherol) are among the medicinally important phytocompounds in *C. thomsoniae*[8]. A sustainable method for the biosynthesis of silver nanoparticles (AgNPs) using *C. thomsoniae* leaf extract is being developed in light of the plant's immense medicinal value. The produced AgNPs were characterized using UV,

Cite this article: Pallab K, Ayodeji O O, Adebola O O. Characterization of Green Synthesized Silver Nanoparticles from *Clerodendrum thomsoniae* Balf.f., and Their Antioxidant and Anti inflammatory Potential. Pharmacogn J. 2025;17(6): 676-682.

scanning electron microscopy (SEM), field emission scanning electron microscopy (FESEM), energy-dispersive X-ray spectroscopy (EDX), and X- ray diffraction (XRD), and their biological potential will be assessed based on their antioxidant and anti-inflammatory properties[7,8].

MATERIAL AND METHODS

Chemicals and Reagents

All reagents and solvents were analytical grades, purchased from Sigma-Aldrich (Pty)Ltd. (Johannesburg, South Africa) and Merck (Pty) Ltd. (Johannesburg, South Africa) through a licensed local supplier, Shalom Laboratories and Supplies, South Africa. Antioxidant absorbance was measured on a 680-BioRad Microplate Reader (Serial Number 14966, Irvine, CA, USA).

Collection and extraction of *Clerodendrum thomsoniae*

Leaves of *C. thomsoniae* were collected in January 2024 from Shivmandir, Siliguri, West Bengal (26.712° N, 88.366° E) after the plant was identified by Pallab Kar (Botanist). The plant was authenticated at the Walter Sisulu University Herbarium situated in the Department of Biological and Environmental Sciences. The voucher number PK/2024/001 was assigned to the herbarium specimen. Fresh *C. thomsoniae* leaves (CT) that had been air-dried for three weeks and were free of disease were ground into a fine powder using a mechanical grinder. Adopting the Soxhlet extraction process, 10 g of crushed leaves were extracted in 70 % methanol (v/v) for 7 h. The extract was concentrated using a rotary evaporator. The extract was then lyophilized to create a dry powder that could be used later.

Synthesis of nanoparticles from silver nitrate (AgNO3) using *C. thomsoniae* leaf extract

Silver nanoparticles (AgNPs) were synthesized by combining AgNO3 [1.575 g (0.103 M) diluted in 90 mL of distilled water] with *C. thomsoniae* leaf extract (30 mg of lyophilized dry powder plant extract dissolved in 10 mL of distilled water). The solution turned from colourless to greyish brown after heating at 80 °C for 6-8 h while being stirred magnetically. Thereafter, the solution was centrifuged for 20 min at room temperature at 10000 rpm (11200 rcf), affording *C. thomsoniae* aqueous extract-based silver nanoparticles (CT-Ag NPs, 1.2 % *w/w*). The samples were stored at 4 °C after air drying[9-11].

Characterization of silver nanoparticles

UV-Visible spectra analysis

Characterization of biogenically synthesized nanoparticles was done by UV-visible spectroscopy on the PerkinElmer UV-Vis absorption spectrometer (PerkinElmer Inc.,Waltham, MA, USA) after 24 h of experiment, and a graph was also plotted.[12]

Scanning electron microscopy (SEM) and field emission scanning electron microscope (FESEM)

The dried powdered samples were placed on copper mesh for SEM and FESEM investigation, and a gold sputtering apparatus was applied with a 3 nm gold coating. SEM (JEOLJSM- IT100InTouchScopeTM, Tokyo, Japan) and FESEM (German manufacturer Carl Zeiss; model: SIGMA-0261) were used to record the surface morphology of the AgNPs at a 5 kV accelerating voltage at 5,500× and 100,000 × magnifications[12].

Energy-dispersive X-ray spectroscopy (EDX)

To determine the presence of elemental Ag, energy dispersive X-ray spectroscopy (EDX) was done using a Scanning Electron Microscope (JEOLJSM-IT100InTouchScopeTM, Tokyo, Japan) equipped with Oxford-EDX software. The powdered dried nanoparticles were mounted on copper mesh, and a 3 nm gold coating was done using a gold sputtering unit. Eighty mm2 SDD detectors that detect elements under high resolution were used for the purpose[12].

X-ray diffraction analysis (XRD)

X-ray diffraction analysis was done using an EMPYREAN machine (Make PAN analytical, Netherlands), equipped with CuKα radiation (λ=1.54584 Å), operated at 40 kv voltage and 30mA current. To determine the crystalline structure, the obtained data were compared with the standard JCPDS library. The average size of crystalline structure has been calculated using the Debye-Scherrer equation: $D = (0.9\lambda/\beta \cos\theta)$, where D is the diameter of crystallite size, λ is the wavelength for CuKα, β is the full width at half-maximum (FWHM), and θ is the Bragg diffraction[9].

Determination of *in vitro* antioxidant activity

Nitric oxide (NO) radical scavenging assay

The quantification technique of the Griess-Ilosvoy reaction at physiological pH was used to measure the nitric oxide radical scavenging activity with minor adjustments.[13] Briefly, phosphate-buffered saline (pH 7.4), sodium nitroprusside (SNP; 10 mM), and different concentrations of silver nitrate (SN), and CT-Ag NPs (0-200 µg/mL) were mixed to make a final volume of 3 mL in three replicates (*n=3*). After the mixture was thoroughly vortexed and incubated for 150 min at 25 °C, 0.5 mL of the pre-incubated reaction mixture was mixed with 1 mL of sulfanilamide (0.33 %), which was diluted in 20 % glacial acetic acid and allowed to it at room temperature for 5 min. To facilitate colour production, 1 mL of N-(1-Naphthyl) ethylenediamine dihydrochloride (NEED; 0.1%) was added, and the mixture was kept at 25 °C for an additional 30 min. Using distilled water as a blank, the absorbance was measured at 540nm. Curcumin functioned as a standard reference. The percent of inhibition was calculated according to the following equation I:

The equation I: $Percentage\ of\ scavenging = (A0 - A1)/A0\ x\ 100$

Where, A0= absorbance of the control and A1= absorbance in the presence of samples and standard.

Hydrogen peroxide scavenging assay

The hydrogen peroxide (H2O2) scavenging capacity was calculated using a modified version of Long et al.[14]. H2O2 (50 mM), different concentrations of silver nitrate (SN), and CT-Ag NPs (0-200 µg/mL) were combined in a screw-capped bottle and incubated in the dark for 30 min at room temperature (≈25 °C). Next, 90 µL of H2O2, 10 µL of HPLC-grade methanol, and 0.9 mL of FOX reagent (made by combining 9 volumes of 4.4 mM BHT in HPLC-grade methanol with 1 volume of 1 mM xylenol orange and 2.56 mM ammonium ferrous sulfate in 0.25 M H2SO4) were added. After giving the mixture a gentle vortex and letting it sit for 30 min, the absorbance at 560 nm was determined. Ascorbic acid was utilized as a positive control. The experiment was conducted in three replicates (n=3). The percentage inhibition was calculated as before using equation I.

Hydroxyl radical scavenging assay

Hydroxyl radical scavenging activity was conducted using the Fenton reaction model with a small modification[15]. 2-deoxy-2-ribose (2.8 mM), monopotassium phosphate-potassium hydroxide buffer (KH2PO4-KOH; 20 mM; pH 7.4), FeCl3 (100 µM), ethylene diamine tetraacetic acid (EDTA; 100 µM), hydrogen peroxide (H2O2; 1.0 mM), ascorbic acid (100 µM), and varying concentrations of silver nitrate (SN), and CT-Ag NPs (0–200 µg/mL) were carefully added to the reaction mixture until a final volume of 1 mL was achieved. Thereafter, the reaction mixture was incubated for 60 min at 37 °C. Then, 0.5 mL mixture was carefully transferred into a fresh tube and mixed with 1

mL each of aqueous thiobarbituric acid (TBA; 1%) and TCA (2.8 %) in three replicates (n=3). The final mixture was incubated for 15 min at 90 °C. The absorbance at 532 nm was measured after the mixture had cooled to room temperature in comparison to an appropriate blank solution. A positive control was employed as ascorbic acid. The percentage inhibition was calculated as before using equation I.

Superoxide radical scavenging assay

The assay was conducted in accordance with Fontana et al.[16]. The nitro-blue tetrazolium (NBT) is reduced to purple formazan in the presence of the nonenzymatic PMS/NADH system, which produces superoxide radicals when exposed to oxygen. Phosphate buffer (20 mM, pH 7.4), NBT (50 µM), PMS (15 µM), NADH (73 µM), and varying doses (0-200 µg/mL) of silver nitrate (SN), and CT-Ag NPs were combined in three replicates (n=3) to create a reaction mixture (1 mL). After gently vortexing the mixtures, they were incubated for 5 min at room temperature. The amount of formazan produced was estimated by measuring the absorbance at 562 nm in comparison to the equivalent blank samples. Quercetin served as a positive control. The percentage inhibition was calculated as before using equation I.

In vitro anti-inflammatory study

The *in vitro* anti-inflammatory properties of silver nitrate (SN), and CT-Ag NPs were determined by their inhibitory effect on protein denaturation using the egg albumin denaturation assay[17] with slight modification. A 0.2 mL of albumin from a fresh chicken egg, 2.8 mL of phosphate buffer saline at pH 6.4, and 2 mL of silver nitrate (SN), and CT-Ag NPs at 12.5, 25, 50, 100, and 200 µg/mL concentrations, were mixed in three replicates (*n=3*). The reaction mixture was incubated at 37 °C for 15 min away from direct light. Then, it was boiled at 70 °C for 5 min in a thermostatic water bath. The resulting mixture was allowed to cool before the absorbance was measured at 655 nm. Diclofenac was used as the reference anti-inflammatory drug. The percentage inhibitory effect of CT-Ag NPs on egg albumin denaturation (EAD) was calculated according to the following equation II:

$$\%\ Inhibition\ of\ EAD = (A0 - A1/Ao\ x\ 100 \qquad (II)$$

Where, EAD = egg albumin denaturation

Statistical analysis

Statistical analysis data are expressed as mean ± SEM (*n*=3); data subjected to statistical analysis by One-way ANOVA with different alphabets in superscript considered significant at $P<0.05$, utilizing the Excel statistical application (Microsoft 365, Microsoft Corporation, USA).

Ethical Standards

All experiments for the study were conducted in adherence to laboratory safety and disposal norms.

RESULTS AND DISCUSSION

UV-Visible Spectroscopy

The visible proof of Ag^+ ion reduction into Ag nanoparticles was the reaction mixture's colour transformation from colourless to yellow and finally to reddish-brown (Figure 1)[18]. Surface Plasmon resonances (SPR) in the 400–500 nm wavelength region is used to verify the production of nanoparticles due to the position, intensity, and width of this SPR peaks, which are highly sensitive to the properties of the nanoparticles and their surrounding medium.[9] In this study, the CT-Ag NPs exhibited an SPR peak at 427 nm, with a nanoparticle size of 65 ± 1.23 nm. This can be described as an SPR peak shift to longer wavelength. In essence, monitoring the shift and shape of the SPR absorption peak using UV-Vis spectroscopy is a standard, effective method to confirm the formation, determine the average size, and assess the stability and aggregation state of silver nanoparticles[19].

Scanning electron microscopy (SEM) and field emission scanning electron microscope (FESEM)

The size and surface morphology of the biosynthesized CT-Ag NPs were primarily assessed by the SEM and FESEM images (Figures 2A and B), which revealed a spherical to cubical shape. Our findings indicate that most CT-Ag NPs are ultrafine articles, measuring less than 100 nm. The average size of NPs is 65 ± 1.23 nm. In certain cases, solvent evaporation or crosslinking during sample preparation may result in the bulking of nanoparticles[20].

X-ray diffraction analysis (XRD)

Several peaks can be seen in the sample's X-ray diffraction (XRD) examination at 38.13^0, 44.33^0, 64.51^0, and 77.35^0. These peaks (111), (200), (220), and (311), in particular, are representative of metallic silver reflections. A sharp peak at 38.12° [reflection index (111)] can be recognized by comparing its values with those provided by the Joint Committee on Powder Diffraction Standards (JCPDS pdf no: 89-3722), which supports the crystalline form of AgNPs. The average size of the nanoparticle is 47 nm, according to Bragg's law and a comparison of this data with the Debye-Scherrer formula (Figure 4)[21].

Determination of *in vitro* antioxidant activity

Anions of superoxide ($O2^{-}$) damage biological macromolecules like proteins and DNA. In vivo, the superoxide anion is a less reactive free radical that can cause the production of more reactive species in situations where oxidative stress is common. At 200 µg/mL, CT-Ag NPs scavenged 55.66 ± 2.57 % of superoxide (IC_{50}=94.5 ± 3.7 µg/mL) (Figure 5A). The relative IC50 values for quercetin were 69.71 ± 2.98. According to the previously mentioned results, the optimized AgNPs made using *Clerodendrum thomsoniae* leaf extract exhibited a potent antioxidant capacity, which can be attributed to the presence of several phytochemicals such tannins, flavonoids, and phenolics. These compounds scavenge free radicals, protecting cells from oxidative damage. At 200 µg/mL, the CT-Ag NPs showed dose-dependent hydroxyl radical scavenging activity (Figure 5B). Although nitric oxide is a necessary signaling molecule, excessive amounts can harm tissues and cells by generating reactive oxygen species (ROS). CT-Ag NPs showed dose-dependent nitric oxide scavenging activity (58.48 ± 1.20 % at 200 µg/mL) in contrast to the standard. Silver nanoparticles and nitric oxide cooperate in living things to stop excessive nitric oxide buildup that could harm membranes (Figure 5C). Hydrogen peroxide is one type of oxygen that is not radical. On rare occasions, nevertheless, it may become toxic and release hydroxyl (OH^-) radicals that are harmful to cells[22]. Thus, its removal is essential to the antioxidant defense system. The results demonstrated that the synthesized AgNPs had a significant dose-dependent H2O2 radical scavenging effect when compared to the standard (Figure 5D). For ascorbic acid and CT-AgNPs, the IC50 values were 22.18 ± 2.68 and 57.76 ± 0.41 µg/mL, respectively. Table 1 lists the specific IC50 values for each of the corresponding *in vitro* antioxidant assays.

Anti-inflammatory activity

In this work, the denaturation method of egg albumin (protein) was used. Protein denaturation is the process by which proteins lose their biological function and structure as a result of inflammation brought on by heat, stress, or certain chemicals. Consequently, it is believed that protein denaturation is an indicator of inflammation[23]. The current work evaluated the inhibitory effect of the biosynthesized AgNPs on the denaturation of proteins and albumin. CT-Ag NPs showed dose-dependent inhibition of protein denaturation, although less potent than diclofenac (Figure 6). The IC50 values for CT-Ag NPs and Diclofenac

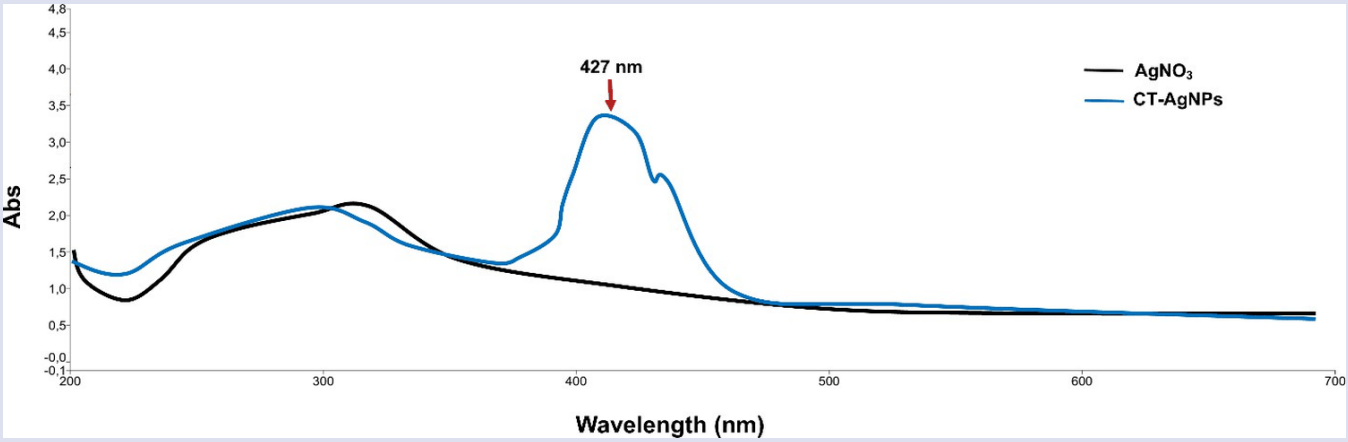

Figure 1. UV-Vis absorption spectrum of CT-Ag NPs, showing a characteristic surface plasmon resonance peak at 427 nm.

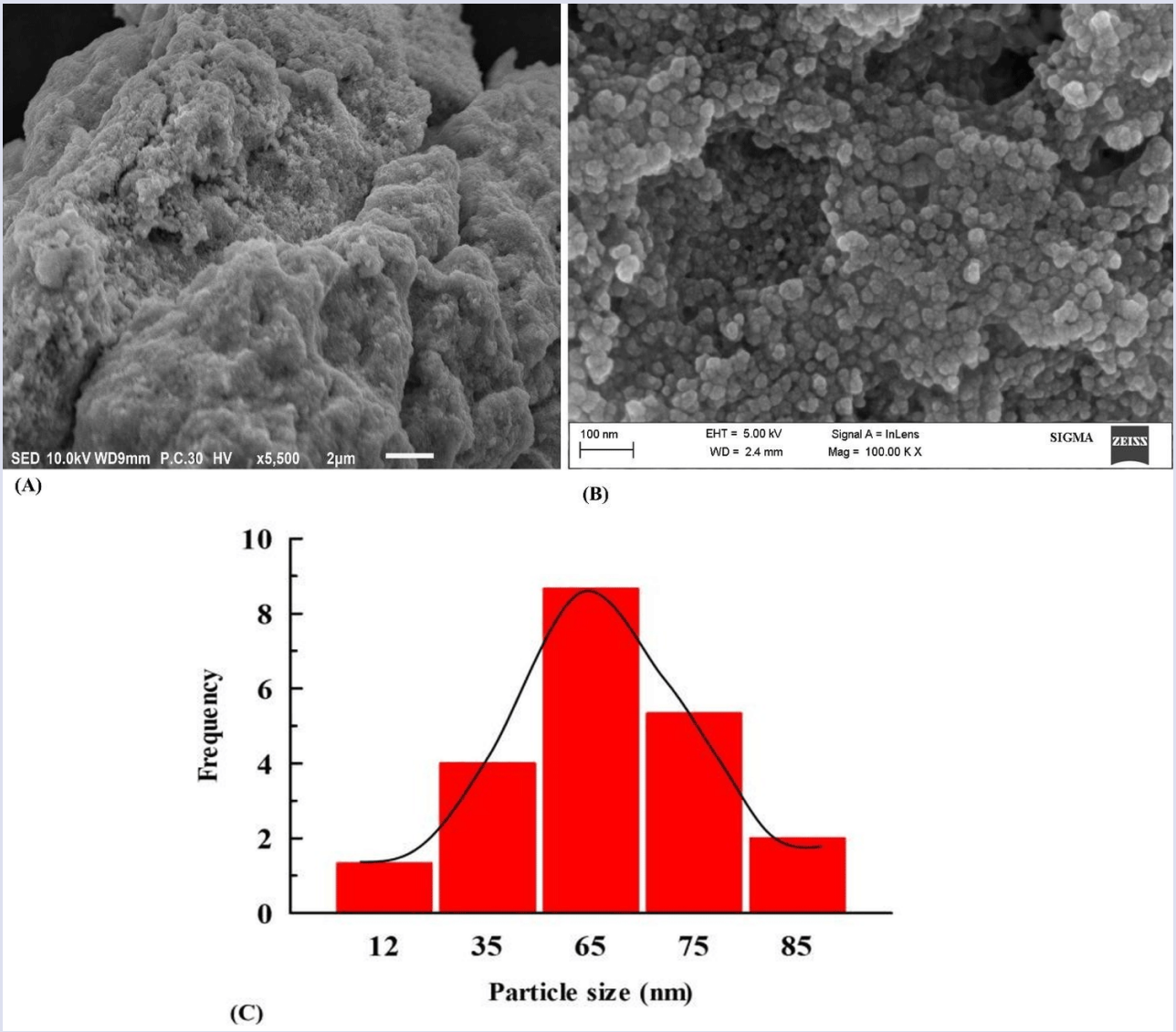

Figure 2. (A) SEM, **(B)** FESEM micrograph, and **(C)** particle size distribution histogram of biosynthesized silver nanoparticles.

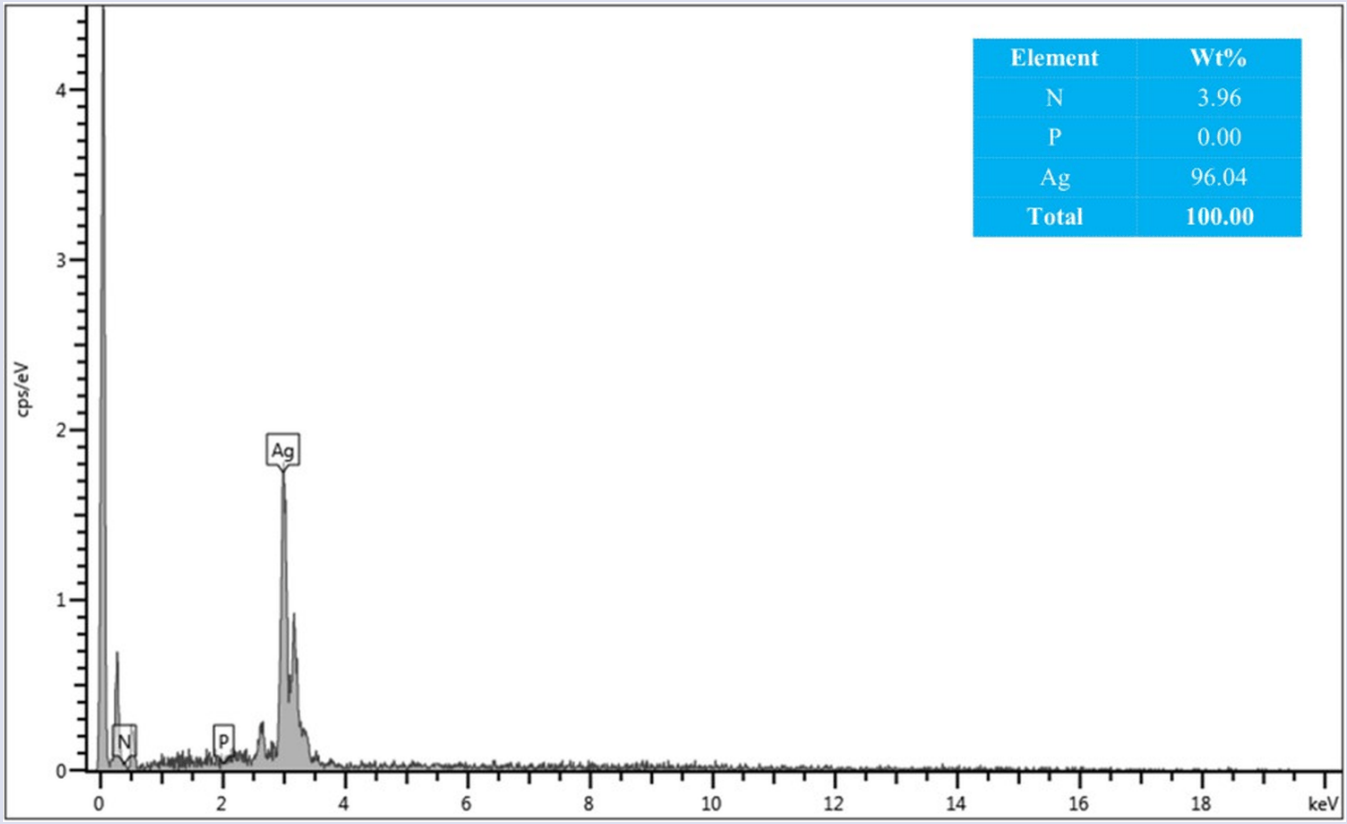

Figure 3. EDX spectra and elemental profile of biosynthesized nanoparticles.

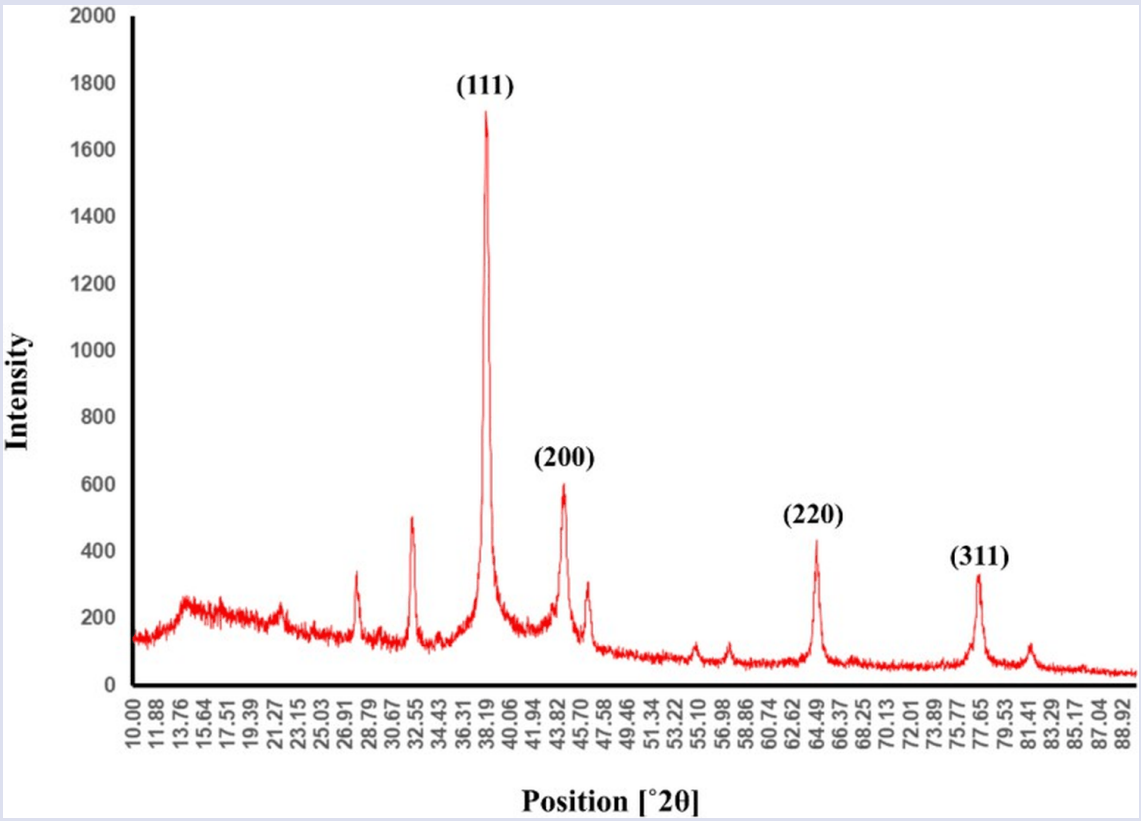

Figure 4. XRD pattern of biosynthesized silver nanoparticles.

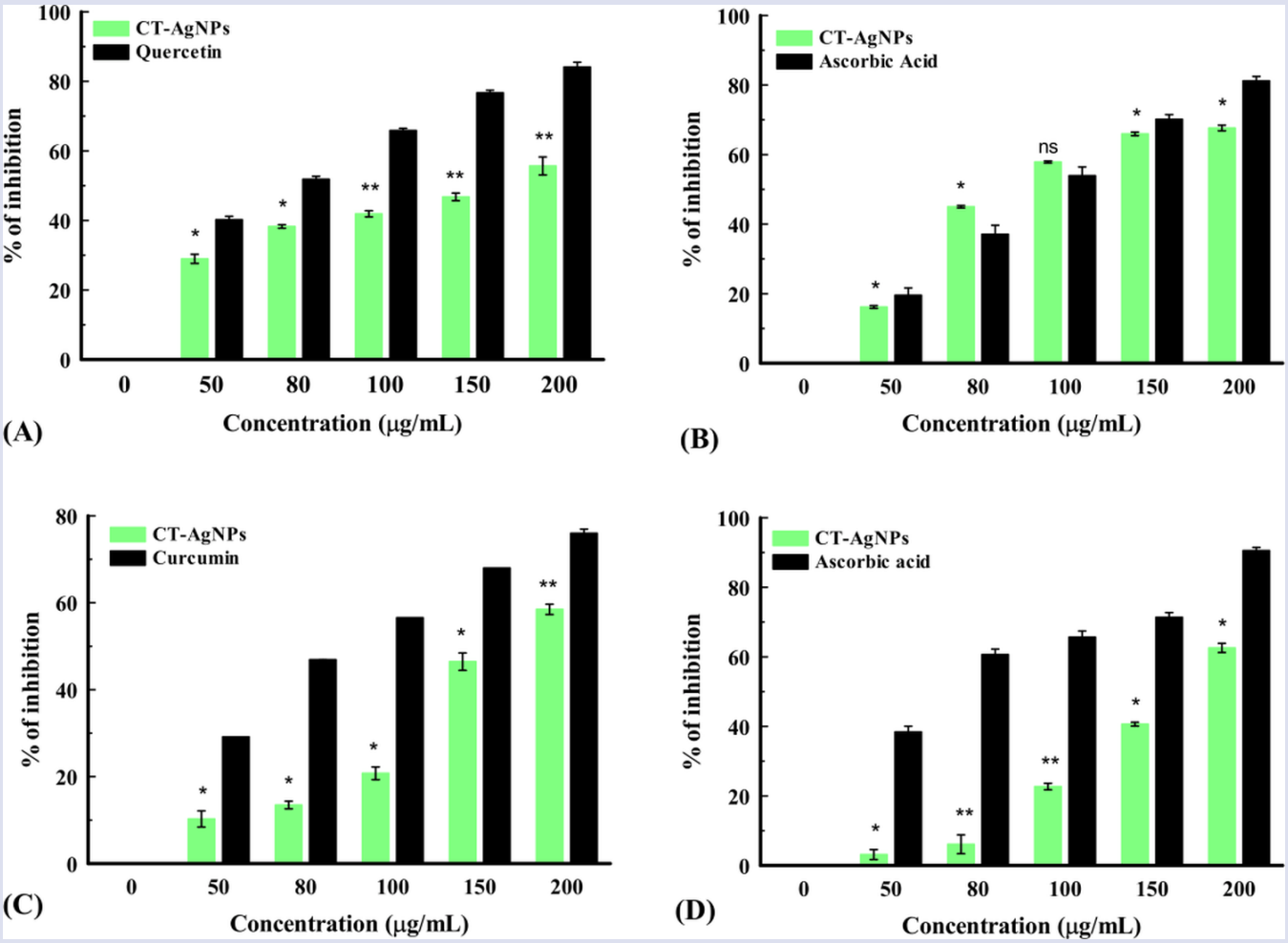

Figure 5. Antioxidant activity of synthesized CT-AgNPs. **(A)** Superoxide radical. **(B)** Hydroxyl radical. **(C)** Nitric oxide. **(D)** Hydrogen peroxide scavenging activity. [Data expressed as mean ± S.D. (*n=3*). *p<0.05; **p<0.01; NS-Non significant when compared with standard drug]. CT-AgNPs: *Clerodendrum thomsoniae* silver nanoparticles.

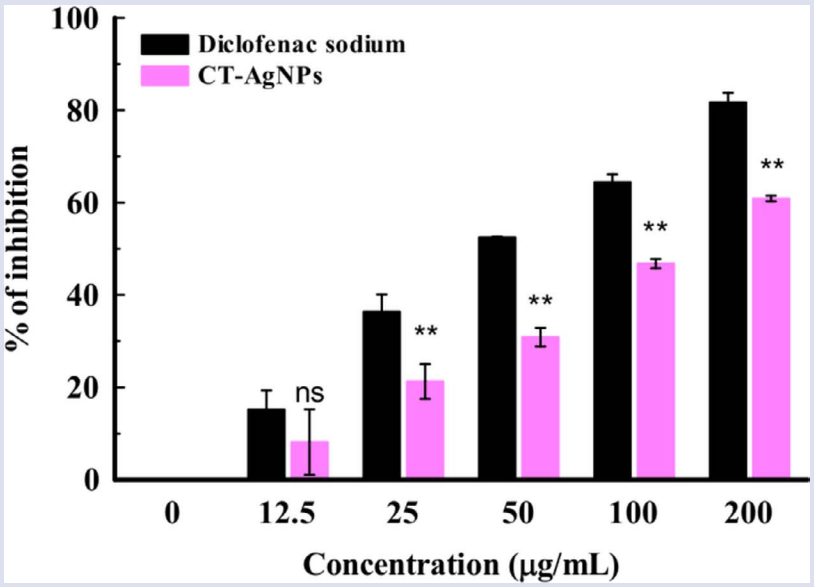

Figure 6. *In vitro* anti-inflammatory activity of the biosynthesized CT-Ag NPs. [Results are given as mean ± S.D. (*n=3*). *p<0.05; **p<0.01; NS-Non-significant when compared with (standard drug)]. CT-AgNPs: *Clerodendrum thomsoniae* silver nanoparticles.

Table 1. IC50 values of CT-Ag NPs and standard drug for different antioxidant assays.

Parameters	CT-AgNPs	Standard drug
Nitric Oxide	64.23 ± 4.21	Curcumin 57.17 ± 0.34
Hydrogen Peroxide	57.76 ± 0.41	Ascorbic acid 22.18 ± 2.68
Hydroxyl Radical	77.81 ± 3.32	Ascorbic acid 62.55 ± 7.41

Table 2. IC50 values of CT-Ag NPs and Diclofenac sodium following in vitro anti-inflammatory test.

Test sample	IC50 ± S.D. (µg/mL)
CT-AgNPs	53.58 ± 17.78
Diclofenac sodium	6.84 ± 1.22

Data expressed as mean ± S.D. (*n=3*). CT-AgNPs: *Clerodendrum thomsoniae* silver nanoparticles, Diclofenac sodium (standard drug)

sodium salt were 53.58 ± 17.78 and 6.84 ± 1.22 µg/mL, respectively (Table 2). AgNPs produced by *A. belladonna* suppressed albumin denaturation with an IC50 value of 84 µM, according to Das *et al.*[20].

CONCLUSION

In this study, the leaf aqueous extract of *C. thomsoniae* upon nanoparticle green synthesis resulted in spherical-to-cubical shaped CT-Ag NPs, with an average size of 47 nm and an elemental silver content of 96.04 %. It scavenged NO, H2O2, superoxide, and hydroxyl radicals in a dose-dependent manner, while also inhibiting protein denaturation. Thus, the notable antioxidant and anti-inflammatory properties of CT-Ag NPs suggest that they show potential for further exploration as bioactive agents. Further studies to evaluate the toxicological profile of CT-Ag NPs on vital organs and the *in vivo* anti-inflammatory effect may be worthwhile.

ACKNOWLEDGMENTS

The authors are grateful to the Research Directorates of Walter Sisulu University (African Medicinal Flora and Fauna Niche Area and PDRFs) and NRF Rated Researcher Incentive for their financial support.

REFERENCES

1. Gaur M, Misra C, Yadav AB, Swaroop S, Maolmhuaidh F, Bechelany M, Barhoum A.Biomedical Applications of Carbon Nanomaterials: Fullerenes, Quantum Dots,Nanotubes, Nanofibers, and Graphene Materials. 2021; 14: 5978.
2. Barhoum A, Pal K, Rahier H, Uludag H, Kim IS, Bechelany M. Nanofibers as new-generation materials: From spinning and nano-spinning fabrication techniques to emerging applications. Appl Mater Today 2019; 17: 1–35.
3. Rassaei L, Marken F, Sillanpaa M, Amiri M, Cirtiu CM, Sillanpaa M. Nanoparticles in electrochemical sensors for environmental monitoring. TrAC Trends Anal Chem. 2011; 30: 1704–1715.
4. Netala VR, Kotakadi VS, Nagam V, Bobbu P, Ghosh SB, Tartte V. First report of biomimetic synthesis of silver nanoparticles using aqueous callus extract of Centella asiatica and their antimicrobial activity. Appl Nanosci. 2015; 5: 801-807.
5. Burdușel AC, Gherasim O, Grumezescu AM, Mogoantă L, Ficai A, Andronescu E. Biomedical applications of silver nanoparticles: an up-to-date overview. Nanomaterials.2018; 8(9): 681.
6. Patel JJ, Acharya SR, Acharya NS. *Clerodendrum serratum* (L.) Moon.–A review on traditional uses, phytochemistry and pharmacological activities. J Ethnopharmacol. 2014; 154(2): 268-285.
7. Shrivastava N, Patel T. *Clerodendrum* and healthcare: an overview. Med Aromat Plant 361 Sci Biotechnol. 2007; 1(1): 142-150.
8. Kar P, Oriola AO, Oyedeji AO. *In vitro* antioxidant, anti-inflammatory, anti-cancer and in silico molecular docking studies of *Clerodendrum thomsoniae*. J Phytol. 2024; 16: 200-215.
9. Banerjee S, Kar P, Sarkar I, Chhetri A, Mishra DK, Dutta A, Kumar A, Sinha B, Sen A. Structural elucidation and chemical characterization of underutilized fruit silverberry (*Elaeagnus pyriformis*) silver nanoparticles playing a dual role as anti-cancer agent by promoting apoptosis and inhibiting ABC transporters. S Afr J Bot. 2022; 145: 243-257.
10. Kar P, Banerjee S, Chhetri A, Sen A. Synthesis, physicochemical characterization and biological activity of synthesized Silver and Rajat Bhasma nanoparticles using *Clerodendrum inerme*. J Phytol. 2021; 1: 64-71.
11. Kar P, Banerjee S, Saleh-E-In MM, Anandraj A, Kormuth E, Pillay S, Al-Ghamdi AA, Ali MA, Lee J, Sen A, Naidoo D, Roy A, Choi YE. β-sitosterol conjugated silver nanoparticle-mediated amelioration of CCl4-induced liver injury in Swiss albino mice. J King Saud Univ Sci. 2022; 34: 102113.
12. Kar P, Oriola AO, Singh M, Oyedeji AO. Myricitrin-Mediated Biogenic Silver Nanoparticle Synthesis, Characterization, and its Antioxidant, Anticancer, and DNA Cleavage Activities. Phcog J. 2025; 17(2): 121-128.
13. Garratt DC. The Quantitative Analysis of Drugs. Chapman and Hall Ltd Springer Japan.1964.
14. Long LH, Evans PJ, Halliwell B. Hydrogen peroxide in human urine: implications for antioxidant defense and redox regulation. Biochem Biophys Res Commun. 1999; 262(3): 605-609.
15. Kunchandy E, Rao MNA. Oxygen radical scavenging activity of curcumin. Int J Pharm. 385 1990; 58(3): 237-240.
16. Fontana M, Mosca L, Rosei MA. Interaction of enkephalins with oxyradicals. Biochem Pharmacol. 2001; 61(10): 1253-1257.
17. Oriola AO, Miya GM, Singh M, Oyedeji AO. Flavonol Glycosides from Eugenia uniflora Leaves and Their In Vitro Cytotoxicity, Antioxidant and Anti-Inflammatory Activities. Sci Pharm. 2023; 91(3): 42.
18. Bose D, Chatterjee S. Antibacterial activity of green synthesized silver nanoparticles using Vasaka (*Justicia adhatoda* L.) leaf extract. Indian J Microbiol. 2015; 55(2): 163-167.
19. Arif M, Raza H, Akhter T. UV-Vis spectroscopy in the characterization and applications of smart microgels and metal nanoparticle-decorated smart microgels: a critical review. RSC Adv. 2024; 14(51): 38120-34.
20. Das P, Ghosal K, Jana NK, Mukherjee A, Basak P. Green synthesis and characterization of silver nanoparticles using belladonna mother tincture and its efficacy as a potential antibacterial and anti-inflammatory agent. Mater Chem Phys. 2019; 228: 310-317.
21. Bhakya S, Muthukrishnan S, Sukumaran M, Muthukumar M. Biogenic synthesis of silver nanoparticles and their antioxidant and antibacterial activity. Appl Nanosci. 2016; 6: 755-766.
22. Kumar RS, Rajkapoor B, Perumal P. Antioxidant activities of *Indigofera cassioides* Rottl. Ex. DC. using various in vitro assay models. Asian Pac J Trop Biomed. 2012; 2(4): 256-261.
23. Altir NKM, Ali AMA, Gaafar ARZ, Qahtan AA, Abdel-Salam EM, Alshameri A, Hodhod MS, Almunqedhi B. Phytochemical profile, in vitro antioxidant, and anti- protein denaturation activities of Curcuma longa L. rhizome and leaves. Open Chem. 2021; 19(1): 945-952.

Cite this article: Pallab K, Ayodeji O O, Adebola O O. Characterization of Green Synthesized Silver Nanoparticles from *Clerodendrum thomsoniae* Balf.f., and Their aAntioxidant and Anti-inflammatory Potential. Pharmacogn J. 2025;17(6): 676-682.